THE JOURNAL OF BIOLOGICAL CHEMISTRY VOL. 285, NO. 45, pp. 34765–34772, November 5, 2010


# FMN Binding and Photochemical Properties of Plant Putative Photoreceptors Containing Two LOV Domains, LOV/LOV Proteins*[S]

Received for publication, May 18, 2010, and in revised form, September 5, 2010 Published, JBC Papers in Press, September 8, 2010, DOI 10.1074/jbc.M110.145367

**Masahiro Kasahara**[1], **Mayumi Torii, Akimitsu Fujita, and Kengo Tainaka**

*From the Department of Biotechnology, College of Life Sciences, Ritsumeikan University, Nojihigashi, Kusatsu, Shiga 525-8577, Japan*

**LOV domains function as blue light-sensing modules in various photoreceptors in plants, fungi, algae, and bacteria. A LOV/LOV protein (LLP) has been found from *Arabidopsis thaliana* (*At*LLP) as a two LOV domain-containing protein. However, its function remains unknown. We isolated cDNA clones coding for an LLP homolog from tomato (*Solanum lycopersicum*) and two homologs from the moss *Physcomitrella patens*. The tomato LLP (*Sl*LLP) contains two LOV domains (LOV1 and LOV2 domains), as in *At*LLP. Most of the amino acids required for association with chromophore are conserved in both LOV domains, except that the amino acid at the position equivalent to the cysteine essential for cysteinyl adduct formation is glycine in the LOV1 domain as in *At*LLP. When expressed in *Escherichia coli*, *Sl*LLP binds FMN and undergoes a self-contained photocycle upon irradiation of blue light. Analyses using mutant *Sl*LLPs revealed that *Sl*LLP binds FMN in both LOV domains, although the LOV1 domain does not show spectral changes on irradiation. However, when $Gly^{66}$ in the LOV1 domain, which is located at the position equivalent to the essential cysteine of LOV domains, is replaced by cysteine, the mutated LOV1 domain shows light-induced spectral changes. In addition, all four LOV domains of *P. patens* LLPs (*Pp*LLP1 and *Pp*LLP2) show the typical features of LOV domains, including the reactive cysteine in each. This study shows that plants have a new LOV domain-containing protein family with the typical biochemical and photochemical properties of other LOV domain-containing proteins such as the phototropins.**

Four photoreceptor families have been found from plants including phytochrome, cryptochrome, phototropin, and ADO/FKF/LKP/ZTL family proteins. Among them, phototropin and ADO/FKF/LKP/ZTL use a common light-sensing domain, LOV domain (1). The LOV domain was found as the light-sensing domain of the phototropin (PHOT1 and PHOT2) (2–4) and has been well characterized (1, 5–7). LOV domain-containing proteins are distributed not only in plants but also in many other organisms. For example, WC-1 and VVD are found in the ascomycete fungus *Neurospora crassa* (8), aureochrome in the alga *Vaucheria frigida* (9), and bacterial histidine kinases in the animal pathogenic bacterium *Brucella abortus* (10) and in the stalked bacterium *Caulobacter crescentus* (11). These proteins have all been shown to function as photoreceptors.

Six genes encoding LOV domain-containing proteins are found in the genome of *Arabidopsis thaliana*. Among them, two encode phototropins, and three encode the ADO/FKF/LKP/ZTL family proteins, proteins involved in circadian clock and photoperiod-dependent flowering functions (12–15). All of the LOV domains of phototropins and ADO/FKF/LKP/ZTL family proteins are shown to bind FMN (2, 4, 15, 16). In addition to those above, there exists a unique LOV domain-containing protein, referred to as PAS/LOV protein (PLP),[2] which contains a PAS domain followed by a LOV domain (1, 17).

Ogura *et al.* (18) screened for proteins interacting with *A. thaliana* PLP using the yeast two-hybrid system. They isolated VTC2 (vitamin C defective 2), VTC2L (VTC2-like), and BLH10A and BLH10B (BEL1-like homeodomain 10 A and B proteins) as interacting proteins in yeast cells. The molecular interactions between PLP and VTC2L, BLH10A, or BLH10B in yeast were dependent on blue light irradiation, suggesting that PLP may function as a photoreceptor (18). Blue light treatment diminished the interaction. However, the flavin binding and photochemical properties of the *A. thaliana* PLP are unclear because the recombinant protein expressed in *Escherichia coli* did not show absorption spectra of flavin-binding proteins (18).

In this study, we isolate cDNAs coding for PLP homologs from tomato (*Solanum lycopersicum*) and the moss *Physcomitrella patens*, and phylogenetic analysis shows that the PAS domains of the homologs, even the PAS domain of *A. thaliana* PLP, are closely related to the LOV domain. Thus, we propose that the isolated LOV domain-containing protein should be referred to as LOV/LOV protein (LLP), instead of PLP. Here, we analyze chromophore binding and photochemical properties of LLP from *S. lycopersicum* using wild-type and mutant proteins expressed in *E. coli*. We also examine both LOV domains of both *Pp*LLPs for FMN binding and photochemical properties.

* This work was supported in part by the Ministry of Education, Sciences and Culture with a Grant-in-Aid for Young Scientists (B) (to M. K.).

[S] The on-line version of this article (available at http://www.jbc.org) contains supplemental Tables S1–S3 and Figs. S1–S3.

*The nucleotide sequence(s) reported in this paper has been submitted to the DDBJ/GenBank™/EBI Data Bank with accession number(s) AB576162, AB576160, and AB576161.*

[1] To whom correspondence should be addressed: 1-1-1 Nojihigashi, Kusatsu, Shiga 525-8577, Japan. Fax: 81-77-561-2659; E-mail: kasa@sk.ritsumei.ac.jp.

[2] The abbreviations used are: PLP, PAS/LOV protein; LLP, LOV/LOV protein.

## EXPERIMENTAL PROCEDURES

*Cloning and Sequencing of SlLLP cDNA*—To obtain tomato LLP cDNA, RT-PCR was performed using total RNA from flowers of tomato (*S. lycopersicum* cv. Micro-Tom). The primers and DNA polymerase used were LLP-S-F and LLP-S-R (supplemental Table S1) and KOD-Plus (Toyobo, Tsuruga, Japan), respectively. The PCR products were inserted into the pGEM-T easy vector (Promega, Madison, WI) after treatment with ExTaq polymerase (Takara, Otsu, Japan) to add dT at the 3′ ends. Two clones were sequenced, and the complete match of the nucleotide sequences was verified between them. The obtained nucleotide sequence has been submitted to GenBank/EMBL/DDBJ Data Bank with accession number AB576162.

*Expression of Recombinant SlLLP in E. coli*—For protein expression of SlLLP, cDNA of SlLLP was amplified by PCR using the two primers LLP-F and LLP-R (supplemental Table S1). The PCR product was digested with XhoI and NotI and cloned into the XhoI-NotI site of pThioHisA plasmid (Invitrogen), and the resulting plasmid was named pThio-*Sl*LLP. The *Sl*LLP recombinant protein is expressed as a fusion protein with His-Patch thioredoxin at the N terminus and $His_6$ at the C terminus. *E. coli* JM109 having pRARE2LysS (Novagen, Madison, WI) that supplies tRNAs for rare codons to enhance the expression of eukaryotic proteins was used for the host cell.

*Purification of Recombinant SlLLP*—The transformants, JM109 cells harboring pThio-*Sl*LLP and pRARE2LysS, were grown overnight at 37 °C in Luria-Bertani medium (30 ml) supplemented with ampicillin (100 $\mu$g ml$^{-1}$) and chloramphenicol (30 $\mu$g ml$^{-1}$). The overnight-cultured cells (20 ml in LB medium) were added to M9 medium (1 liter) supplemented with ampicillin (100 $\mu$g ml$^{-1}$) and chloramphenicol (30 $\mu$g ml$^{-1}$) and were grown at 25 °C to an optical density (600 nm) of ~0.35. Protein expression was carried out for 20 h at 20 or 25 °C in the presence of 1.5 mM isopropyl $\beta$-D-thiogalactopyranoside. The cells were harvested by centrifugation, frozen at −80 °C, thawed at 25 °C, and then resuspended in 20 ml of a disruption solution (20 mM Tris-HCl, pH 8.0, 0.5 M NaCl, 5 mM 2-mercaptoethanol, 20 mM imidazole) with 0.2% (w/v) Tween 60. After sonication for disruption, the cell extract was centrifuged at 35,000 × *g* for 30 min at 4 °C. The supernatant was loaded onto a nickel-Sepharose 6 Fast Flow column (1 ml of bed volume; GE Healthcare). The column was washed twice with 10 ml of the disruption solution with 0.2% (w/v) Tween 60, twice with 10 ml of the disruption solution, and then once with 5 ml of the disruption solution with 75 mM imidazole. The protein was eluted with 3 ml of the disruption solution with 200 mM imidazole. The eluate was added to 9 ml of a buffer solution (20 mM Tris-HCl, pH 8.0) and loaded onto a HiTrapQ column (GE Healthcare). The column was washed with the buffer solution with 0.15 M NaCl, and then the protein was eluted with a linear NaCl gradient (0.15–0.8 M).

*Site-directed Mutagenesis*—Mutant versions of pThio-*Sl*LLP were generated by PCR-based site-directed mutagenesis (19). Mismatch primers used for the PCR are listed in supplemental Table S1. The resulting PCR products were mixed and used as templates for next PCR using LLP-F and LLP-R primers. PCRs were performed with KOD-Plus DNA polymerase (Toyobo). The resulting PCR products were cloned into pThioHisA (Invitrogen). pThio-*Sl*LLP-C295A, -R67D, and -R296D were used for protein expression of *Sl*LLP-C295A, -R67D, and -R296D, respectively. To express *Sl*LLP-R67D/R296D, the 5.2- and 0.4-kb MunI-XbaI fragments of pThio-*Sl*LLP-R67D and pThio-*Sl*LLP-R296D, respectively, were ligated. The resulting pThio-*Sl*LLP-R67D/R296D was used for *Sl*LLP-R67D/R296D expression. To express *Sl*LLP-G66C/R296D, the pThio-*Sl*LLP-G66C/R296D plasmid was constructed using mismatch primers (supplemental Table S1) and pThio-*Sl*LLP-R296D as a template. PCR and cloning into the pThioHisA plasmid were performed as described above.

*Expression and Purification of Recombinant PpLLP1 and PpLLP2 and Each LOV Domain in E. coli*—For protein expression, cDNAs were amplified by PCR using the two primers listed in supplemental Table S1. The PCR products were digested with EcoRI and XhoI and cloned into the EcoRI-XhoI site of pGEX-6P-1 plasmid (GE Healthcare), and the resulting plasmids were introduced into *E. coli* Rosetta2 (DE3) pLysS (Novagen, Madison, WI). The transformants were grown overnight at 37 °C in Luria-Bertani medium (10 ml) supplemented with ampicillin (100 $\mu$g ml$^{-1}$) and chloramphenicol (30 $\mu$g ml$^{-1}$). The overnight-cultured cells (4 ml in LB medium) were added to LB medium (0.5 liter) supplemented with ampicillin (100 $\mu$g ml$^{-1}$) and chloramphenicol (30 $\mu$g ml$^{-1}$) and were grown at 25 °C to an optical density (600 nm) of ~0.5. Protein expression was carried out for 20 h at 20 °C in the presence of 0.5 mM isopropyl $\beta$-D-thiogalactopyranoside. The cells were harvested by centrifugation, frozen at −80 °C, thawed at 25 °C, and then resuspended in 25 ml of a disruption solution (20 mM Tris-HCl, pH 8.0, 5% (w/v) glycerol, 0.1 M NaCl, 10 mM 2-mercaptoethanol, 1 mM EDTA) with 0.2% (w/v) Triton X-100. After sonication for disruption, the cell extract was centrifuged at 35,000 × *g* for 30 min at 4 °C. The supernatant was loaded onto a glutathione-Sepharose 6 column (0.7 ml of bed volume; GE Healthcare). The column was washed twice with 10 ml of the disruption solution with 0.2% (w/v) Triton X-100 and twice with 10 ml of the disruption solution. The proteins were eluted with the disruption solution with 10 mM glutathione. The nucleotide sequences have been submitted to the GenBank/EMBL/DDBJ Data Bank with accession numbers AB576160 (*PpLLP1*) and AB576161 (*PpLLP2*).

*Spectral Analysis*—Absorption spectra for recombinant proteins were obtained using a spectrophotometer (Multispec-1500; Shimadzu, Kyoto, Japan). For light-induced absorption changes, the samples were irradiated with blue light for 10 s at 600 $\mu$mol m$^{-2}$ s$^{-1}$, and the spectra were recorded at 25 °C at regular intervals as described in the figure legends. For light-induced absorption changes of *Sl*LLP-R67D, the sample was centrifuged briefly to remove any aggregates from the protein solution before measuring spectra. A high power blue LED (LXHL-LB3C; Phillips Lumileds, CA) was used as a light source for the light irradiation. The fluence rates were measured using a quantum sensor (LI-250A; LI-COR, Lincoln, NE).

*Other Analytical Procedures*—Protein concentrations were determined by the method of Bradford as described in the instructions accompanying the Bio-Rad protein assay kit with $\gamma$-globulin as a standard. To determine the concentration of

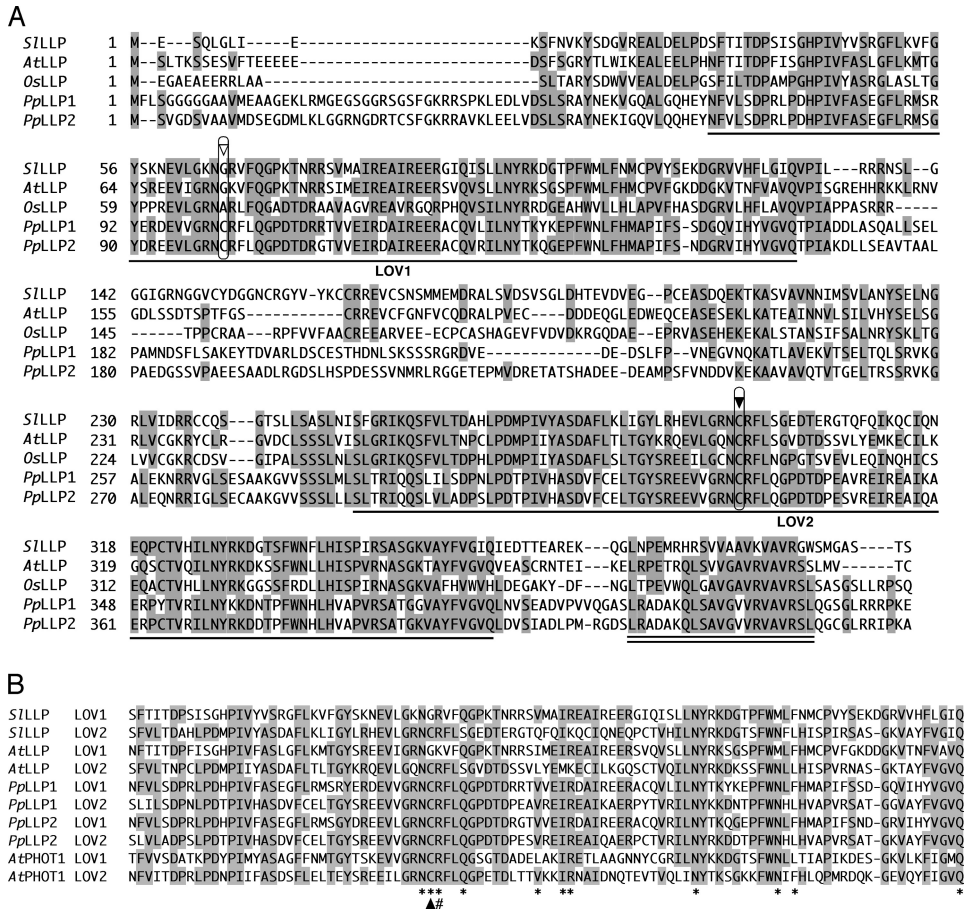


FIGURE 1. **Amino acid alignments of LLPs.** *A*, alignment of the amino acid sequences of full-length LLPs of *S. lycopersicum*, *A. thaliana*, *O. sativa*, and *P. patens*. Amino acid residues identical in more than three sequences are *shaded*. Gaps introduced for good alignment are indicated by *dashes*. The *numbers* are the amino acid positions for each amino acid sequence. *Single lines* indicate LOV1 and LOV2 domains. The highly conserved cysteines in the LOV2 domains are indicated by the *solid arrowhead*. The corresponding amino acids in the LOV1 domains are indicated by the *open arrowhead*. A highly conserved C-terminal region is indicated by a *double line*. *B*, alignment of LOV domains of LLPs with LOV domains of *A. thaliana* PHOT1. Amino acid residues involved in association with FMN, as deduced from the crystal structure of a phototropin LOV domain (21), are indicated by *asterisks*. The highly conserved cysteines in LOV domains are indicated by a *solid arrowhead*. Arginines that we replaced with aspartates in this study are indicated by #.

the homologs were obtained by RT-PCR and sequenced. The deduced amino acid sequences are shown in Fig. 1*A* and aligned with *At*PLP and the homologous sequence in *Oryza sativa* (rice), which is from the rice genome database. Approximately 100 amino acids in N- and C-terminal regions showed high similarity (Fig. 1*A*, *underlining*). Phylogenetic analysis of those amino acid sequences with various PAS domain sequences clearly showed that all of the sequences including the PAS domain of *At*PLP were clustered with LOV domains of phototropins (Fig. 2), as is the case with a former phylogenetic analysis (20). Thus, we propose that the isolated LOV domain-containing protein and *At*PLP should be referred to as LLP, instead of PLP. The *S. lycopersicum* homolog is named *Sl*LLP, and the two *P. patens* homologs are named *Pp*LLP1 and *Pp*LLP2, and the N-terminal and the C-terminal LOV domains are named LOV1 and LOV2 domains, respectively (Fig. 1*A*). A highly conserved short region was found in the C terminus (Fig. 1*A*, *double underlining*).

Fig. 1*B* compares the amino acid sequences of the LOV1 and LOV2 domains of LLPs with those of the LOV domains of *A. thaliana* phototropin 1 (Fig. 1*B*). Most of the conserved amino acids that are associated with flavin binding (21) are conserved in both LOV domains of LLPs (*asterisks* in Fig. 1*B*). However, the amino acids at the position of the cysteine that is essential for photoproduct formation in LOV domains are different in the LOV1 domains of *A. thaliana* (glycine), *O. sativa* (alanine), and *S. lycopersicum* (glycine) LLPs (Fig. 1, *A*, open *arrowhead*, and *B*, *arrowhead*).

FMN associated with *Sl*LLP, purified protein samples were denatured by treatment with 1% SDS, and the concentrations of the released FMN were calculated by using a series of FMN standards as described by Christie *et al.* (2).

## RESULTS

*Cloning of cDNAs Coding for LLP from S. lycopersicum and P. patens and Sequence Homology*—To examine whether *A. thaliana* PLP (*At*PLP) binds flavin as chromophore and shows a LOV domain photocycle, we tried to produce recombinant protein of *At*PLP in *E. coli*. However, it was difficult to find optimal conditions to express a sufficient amount of the recombinant protein because of its high insolubility and low protein expression level, as was the case in another study (18). Thus, we decided to try to express homologs of *At*PLP in *E. coli*.

Using the amino acid sequence of *At*PLP as a query in a BLAST search on a tomato (*S. lycopersicum*) EST database (MiBASE, Kazusa DNA Research Institute) and the *P. patens* genome database (JGI), we found one homolog from *S. lycopersicum* and two homologs from *P. patens*. The cDNAs coding for

*FMN Binding of SlLLP*—To characterize the properties of flavin binding and photocycle of *Sl*LLP, a fusion protein of *Sl*LLP with His-Patch thioredoxin at the N terminus and $His_6$ at the C terminus was expressed in *E. coli*. The His-Patch thioredoxin and $His_6$ were fused to facilitate the purification of the fusion protein by affinity chromatography on a nickel-agarose column.

The *Sl*LLP was purified to near homogeneity by affinity chromatography and anion exchange chromatography (Fig. 3*A*, *arrowhead*). The estimated molecular mass (56.4 kDa) by SDS-PAGE was in agreement with the theoretical values (58.8 kDa) from the amino acid sequences. The 56.4-kDa polypeptide was recognized by both anti-thioredoxin and anti-$His_6$ antibodies (data not shown). Minor lower molecular mass polypeptides

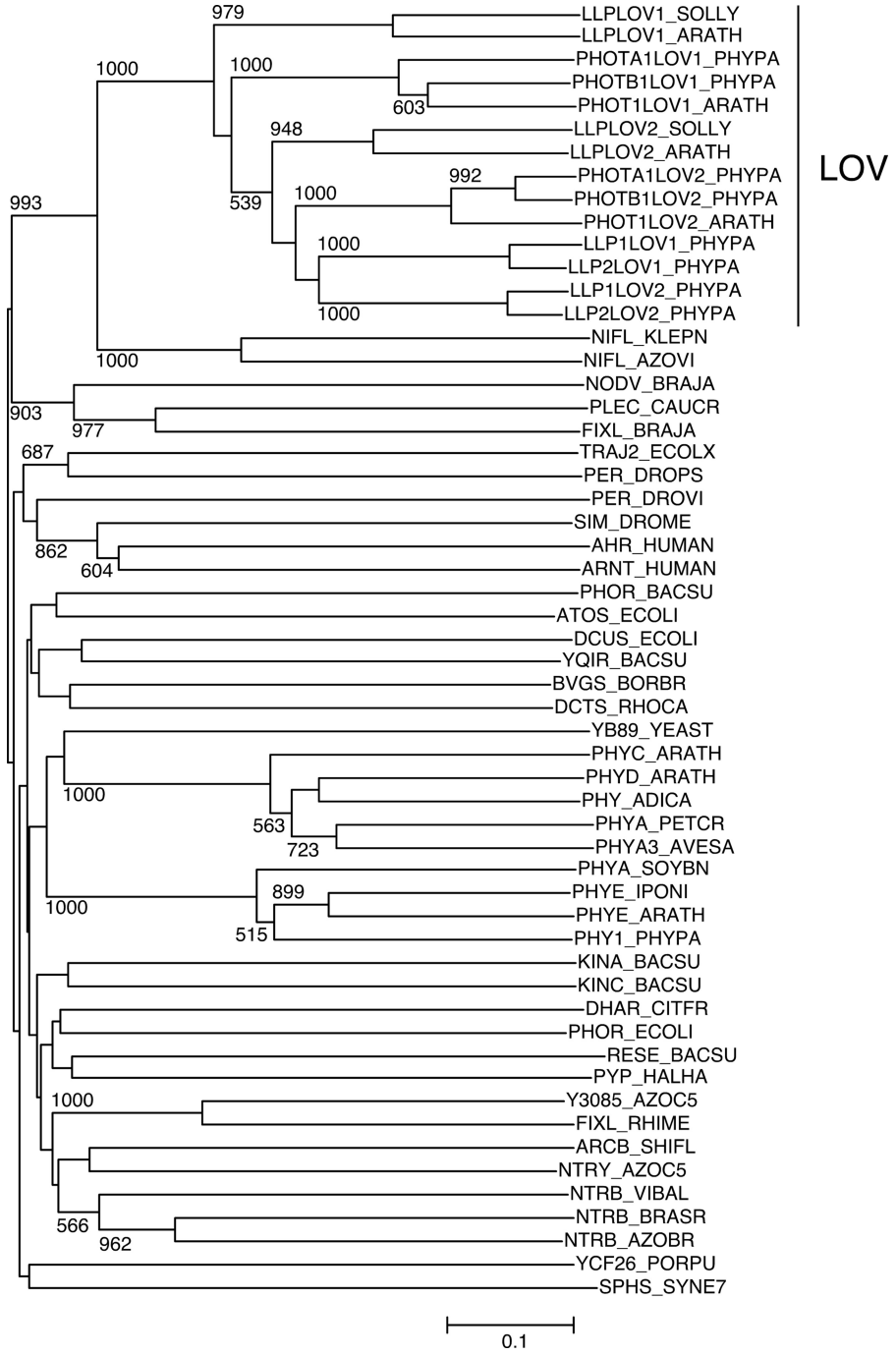


FIGURE 2. **Phylogenetic tree of LOV domain sequences of LLPs with PAS domain superfamily sequences.** The tree was constructed by the NJ method after ClustalX alignment of the amino acid sequences of LOV domains of LLPs and PAS domains. Bootstrap values in the NJ analysis were carried out based on 1,000 replications using ClustalX. Bootstrap values higher than 50% are shown for each clade. The scale indicates 0.1 nucleotide substitutions/site. PAS domain sequences were collected from the PF00989 family of the Pfam protein families database (28). LOV domain sequences were used from phototropin 1 (*PHOT1*) of *A. thaliana* (*ARATH*), phototropin A1 and B1 (*PHOTA1* and *PHOTB1*) of *P. patens* (*PHYPA*), and LLPs of *S. lycopersicum* (*SOLLY*), *A. thaliana* (*ARATH*), and *P. patens* (*PHYPA*).

(32.9 and 30.0 kDa; Fig. 3*A*, *asterisks*) likely result from *Sl*LLP degradation because the polypeptides were recognized by either anti-thioredoxin or anti-$His_6$ antibodies, respectively, but not both (data not shown).

The purified *Sl*LLP exhibited features of LOV domains described previously for phototropin and other LOV domain-containing proteins (2, 4, 15), with absorption peaks in the UV-A and blue regions of the spectra and prominent vibrational bands in the blue (Fig. 3*B*). The flavin associated with *Sl*LLP was identified as FMN by thin layer chromatography, according to its mobility against standard FAD, FMN, and riboflavin samples (supplemental Fig. S1). The molar ratio of FMN to protein was 0.37 for *Sl*LLP (supplemental Table S2), although it was expected that the molar ratio will become ~2 because *Sl*LLP contains two LOV domains.

*FMN-Cysteinyl Adduct Formation of SlLLP upon Light Irradiation*—Irradiation of *Sl*LLP with strong blue light induced a decrease of absorption in the blue region of flavin absorption (~450 nm). During a subsequent dark incubation, the blue absorption was restored to the initial state (Fig. 4*A*). Three isosbestic points present at 322, 388, and 405 nm suggest that the light-induced absorption change is the consequence of FMN-cysteinyl adduct formation (3), not that of the photoreduction that occurs in many flavoproteins. A mutant *Sl*LLP (*Sl*LLP-C295A) was investigated because $Cys^{295}$ in LOV2 domain (Fig. 1*A*, *arrowhead*) is likely the residue to form the FMN-cysteinyl adduct. The *Sl*LLP-C295A did not exhibit any absorption change on irradiation with strong blue light (Fig. 4*B*). These properties indicate that an FMN-cysteinyl adduct was formed upon irradiation with blue light in *Sl*LLP, as is the case with the LOV domain of phototropin, and $Cys^{295}$ in the LOV2 domain of *Sl*LLP is the site of FMN-cysteinyl adduct formation.

*Effect of Imidazole on the Rate of Dark Reversion of SlLLP*—We noticed that when samples after nickel-Sepharose 6 Fast Flow column, which contain 200 mM imidazole added to elute recombinant protein from the column, were used for analyzing light-induced absorption changes, the half-life of photoproduct became very short compared with samples excluding imidazole by ion exchange chromatography. Fig. 5 shows the effect of imidazole on the rate of dark reversion of photoproduct. The half-lives of photoproduct under conditions with and without imidazole were 61.4 s and 65.4 min, respectively (Fig. 5). The rate of dark reversion became ~64-

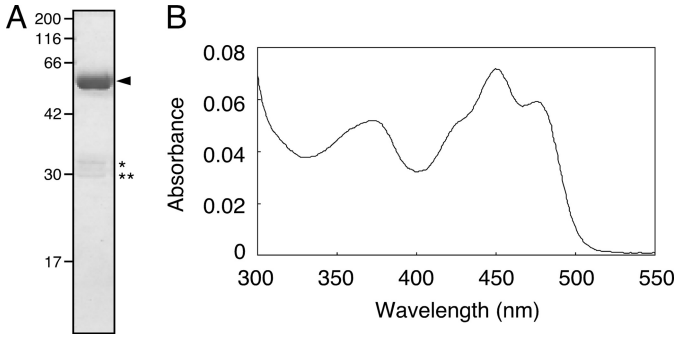


FIGURE 3. **Purification and absorption spectrum of *Sl*LLP.** *A*, SDS-PAGE was carried out using a 12% polyacrylamide gel. The gel was stained with Coomassie Brilliant Blue R250. The *arrowhead* indicates the position of *Sl*LLP. The molecular sizes (in kDa) are indicated on the *left side*. The *asterisks* indicate degradation products of *Sl*LLP. *B*, absorption spectrum of *Sl*LLP.

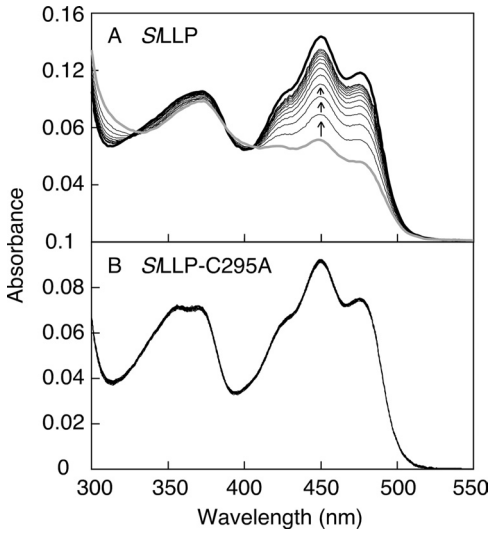


FIGURE 4. **Light-induced absorption change and dark recovery of *Sl*LLP and *Sl*LLP-C295A.** *Sl*LLP (*A*) and *Sl*LLP-C295A (*B*) were irradiated with high intensity blue light (600 $\mu$mol m$^{-2}$ s$^{-1}$) for 10 s. The uppermost spectra (*black heavy lines*) and the lowermost spectra (*gray heavy lines*) at 450 nm represent the initial dark spectra and the spectra immediately after irradiation, respectively, of *Sl*LLP and *Sl*LLP-C295A. All of the spectra of *Sl*LLP-C295A are the same because there was no absorption change on irradiation. After the onset of irradiation, the spectra were recorded at 30-min intervals (total time, 360 min) for *Sl*LLP and 20-s intervals (total time, 160 s) for *Sl*LLP-C295A. The *arrows* indicate the absorption changes with time in the subsequent dark incubation.

fold faster in the presence of imidazole. The imidazole-dependent acceleration of dark reversion was also seen in cyanobacterial LOV domains (22) and the LOV2 domain of oat phototropin 1 (23).

*Analyses of FMN Binding and Photochemical Properties of the LOV1 Domain of SlLLP Using Site-directed Mutagenized Proteins*—The loss of light-induced absorption changes by replacement of Cys$^{295}$ in the LOV2 domain of *Sl*LLP shows that the LOV2 domain is an FMN-binding site. However, it is unclear whether the LOV1 domain binds FMN. To investigate whether the LOV1 domain of *Sl*LLP binds FMN, we constructed a truncated form of *Sl*LLP consisting of the LOV1 domain alone as well as that consisting of the LOV2 domain alone. However, both truncated proteins were expressed as insoluble protein. The full-length polypeptide seems to be required for expression in a soluble form. We tried to express a

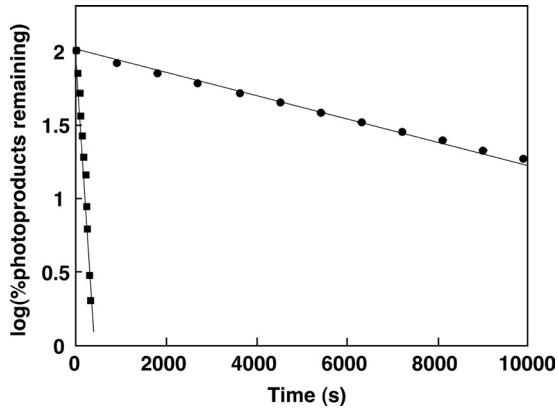


FIGURE 5. **Effect of imidazole on dark reversion kinetics of *Sl*LLP.** The amount of photoproduct remaining after dark incubation is plotted against the duration of dark incubation in the presence (*square*) or the absence (*circle*) of 100 mM imidazole.

full-length *Sl*LLP with a point mutation, by which the mutant protein is considered to dissociate FMN from the LOV2 domain, so that the potential flavin binding site remaining in the mutant protein would be the LOV1 domain. A candidate position of the point mutation was Arg$^{296}$, next to the indispensable cysteine for photoreaction (Fig. 1*B*, #), because the arginine next to the cysteine in LOV domains has been shown to interact with the phosphate group of FMN by forming a salt bridge (21, 24), and point mutations of the arginine result in a complete loss of FMN binding (3).

*SlLLP-R296D*—The *Sl*LLP-R296D, in which Arg$^{296}$ was replaced by aspartate, was constructed. Fig. 6*A* shows the absorption spectrum of the *Sl*LLP-R296D, which was similar to those of LOV domains. However, no absorption change upon blue light irradiation was observed (Fig. 6*B*). Flavin released from *Sl*LLP-R296D showed the same mobility as standard FMN in a TLC analysis. Thus, FMN is suggested to bind to the LOV1 domain, but the LOV1 domain did not undergo the typical photocycle of LOV domains on the time scale of 0.1 s, probably because the LOV1 domain contains a glycine at the position equivalent to the conserved cysteine essential for FMN-cysteinyl adduct formation in LOV domains (Fig. 1*B*, *arrowhead*).

*SlLLP-R67D/R296D*—Next, we constructed a mutant *Sl*LLP, *Sl*LLP-R67D/R296D, in which Arg$^{67}$ in the LOV1 domain was replaced by aspartate in addition to the R296D replacement. We expected that the LOV1 domain would fail to bind FMN as a consequence of the R67D mutation because the Arg$^{67}$ in the LOV1 domain is equivalent to Arg$^{296}$ in the LOV2 domain (Fig. 1*B*, #). Fig. 6*C* shows the absorption spectrum of *Sl*LLP-R67D/R296D. It lacks all but a minor absorption peak in the blue region, showing that *Sl*LLP-R67D/R296D did not bind FMN, and the R67D replacement resulted in a loss of FMN binding. This result indicates that the LOV1 domain in *Sl*LLP binds FMN.

*SlLLP-G66C/R296D*—We constructed a mutant *Sl*LLP, *Sl*LLP-G66C/R296D, in which Gly$^{66}$ in the LOV1 domain (Fig. 1*A*, *open arrowhead*) was replaced by cysteine in the R296D background. We expected that the G66C replacement might generate LOV domain photochemistry for the LOV1 domain because Gly$^{66}$ is located at the position corresponding to the cysteine essential for photochemistry in the LOV domain. The

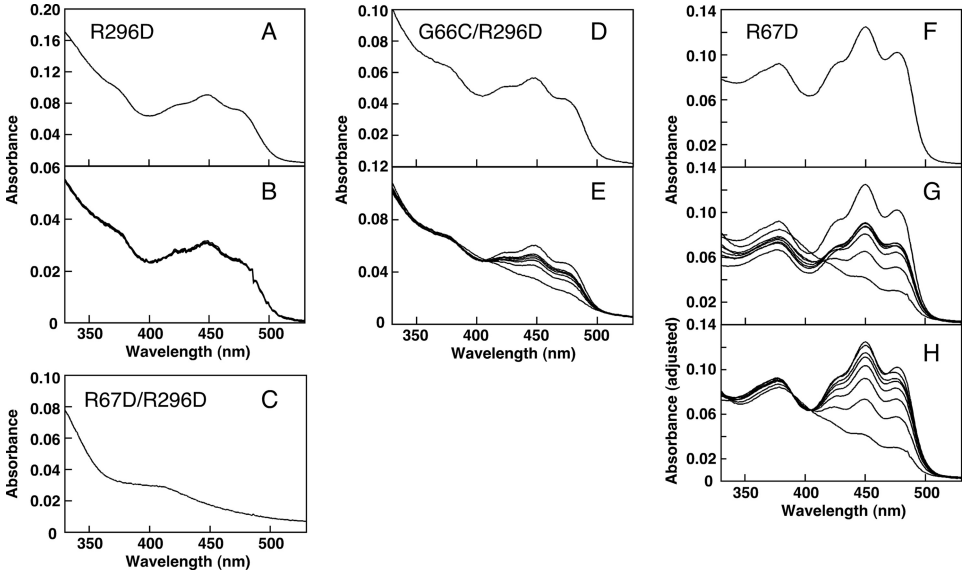


FIGURE 6. **Absorption spectra and absorption change and recovery of *Sl*LLP-R296D, *Sl*LLP-R67D, and *Sl*LLP-R67D/R296D.** *A*, absorption spectrum of *Sl*LLP-R296D. *B*, the uppermost spectrum represents the initial dark spectrum of *Sl*LLP-R296D. After the onset of blue light irradiation (600 $\mu$mol $m^{-2}$ $s^{-1}$) for 10 s, the spectra were recorded at 0.1-s intervals (total time, 1 s). *C*, absorption spectrum of *Sl*LLP-R67D/R296D. *D*, absorption spectrum of *Sl*LLP-G66C/R296D. *E*, the *uppermost* and the *bottom spectra* represent the initial dark spectrum of *Sl*LLP-G66C/R296D and the spectrum right after irradiation with blue light (600 $\mu$mol $m^{-2}$ $s^{-1}$, 10 s), respectively. The spectra after 85, 170, 250, 320, and 395 s (from *bottom* to *top*) are shown. *F*, absorption spectrum of *Sl*LLP-R67D. *G*, the *uppermost* and the *bottom spectra* represent the initial dark spectrum of *Sl*LLP-R67D and the spectrum right after irradiation with blue light (600 $\mu$mol $m^{-2}$ $s^{-1}$, 10 s), respectively. The spectra after 60, 120, 180, 240, 360, and 480 min (from *bottom* to *top*) are shown. *H*, spectra in *E* are normalized in each case to the value of the 405-nm isosbestic point.

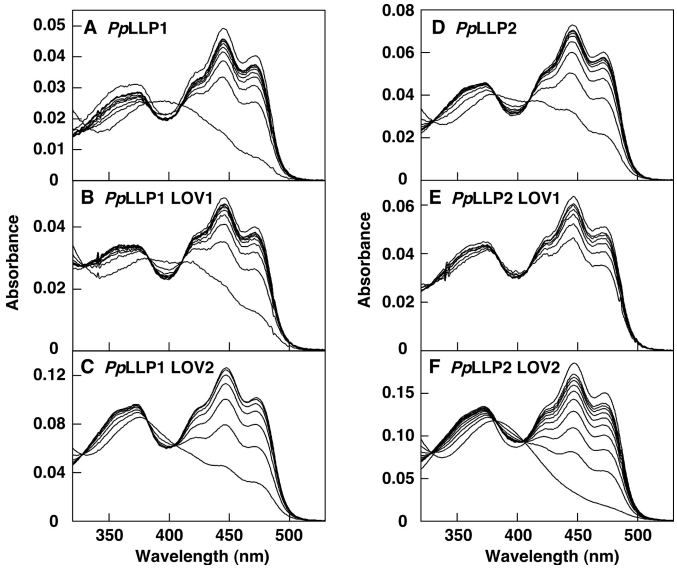


FIGURE 7. **Light-induced absorption change and dark recovery of *Pp*LLP1 and *Pp*LLP2.** Recombinant protein of *Pp*LLP1 (*A*), *Pp*LLP2 (*D*), or each LOV domain (*B*, *C*, *E*, and *F*) were irradiated with high intensity blue light (600 $\mu$mol $m^{-2}$ $s^{-1}$) for 10 s. The *uppermost spectrum* in each panel at 450 nm represent the initial dark spectra. After the onset of irradiation, the spectra were recorded at 6-min intervals (*A*), 10-s intervals (*B*), 9-min intervals (*C*), 1-min intervals (*D*), 1-s intervals (*E*), and 10-min intervals (*F*).

absorption spectrum of *Sl*LLP-G66C/R296D was similar to that of *Sl*LLP-R296D (Fig. 6, *A* and *D*). *Sl*LLP-G66C/R296D showed an absorption change upon blue light irradiation and a subsequent dark recovery (Fig. 6*E*). Three isosbestic points are present at 343, 384, and 406 nm. The light-induced absorption change is likely the consequence of FMN-cysteinyl adduct formation with the Cys[66]. The single G66C amino acid replacement confers photochemistry to the LOV1 domain.

*SlLLP-R67D*—*Sl*LLP-R67D, in which Arg[67] in the LOV1 domain was replaced by aspartate (Fig. 1*B*, #), showed the typical spectrum of a LOV domain (Fig. 6*F*). When measuring light-induced absorption changes and dark recovery of *Sl*LLP-R67D, we observed aggregation in the protein solution. To reduce and remove the aggregation, 5% (w/v) glycerol was added to the protein solution, and the protein solution was centrifuged before measuring each time spectrum. Fig. 6*G* shows the absorption change upon irradiation of blue light and subsequent dark recovery of *Sl*LLP-R67D. The absorption decrease was not restored to the initial state (Fig. 6*G*), probably because of the removal of the aggregated protein and the consequent decrease in the concentration of *Sl*LLP-R67D. When each absorption spectrum was expanded to have the same absorbance at 405 nm (one of the isosbestic points of *Sl*LLP), spectral changes of *Sl*LLP-R67D became similar to those of wild-type *Sl*LLP (compare Figs. 4*A* and 6*H*). The absorbances at 450 nm of *Sl*LLP-R67D and wild-type *Sl*LLP were decreased to 33 and 49% of those of the initial non-light-irradiated forms, respectively (Figs. 4*A* and 6*H*), showing that the relative amount of FMN involved in the light-induced absorption change in *Sl*LLP-R67D is higher than that in wild-type *Sl*LLP. The replacement of Arg[67] resulted in dissociation of FMN bound to the LOV1 domain and increased in the relative amount of FMN able to form the FMN-cysteinyl adduct in *Sl*LLP-R67D. This result also shows that the LOV1 domain in *Sl*LLP binds FMN.

*FMN Binding and Photochemical Properties of P. patens LLPs, PpLLP1 and PpLLP2*—To characterize the properties of flavin binding and photocycle of *Pp*LLP1 and *Pp*LLP2, the full-length proteins and each of the four LOV domains were expressed in *E. coli* as GST fusion proteins. Full-length *Pp*LLP1 and *Pp*LLP2 and LOV domains of *Pp*LLP1 (*Pp*LLP1LOV1 and *Pp*LLP1LOV2) and *Pp*LLP2 (*Pp*LLP2LOV1 and *Pp*LLP2LOV2) were purified by affinity chromatography. FMN was detected by a thin layer chromatography from *Pp*LLP1 and *Pp*LLP2 (supplemental Fig. S1). Fig. 7 shows absorption spectra and spectral changes upon blue light irradiation. All of the purified recombinant proteins exhibited spectral features of LOV domain-containing protein, *i.e.* absorption peaks in the UV-A and blue regions, light-induced absorption change, and having three isosbestic points during the absorption change (Fig. 7). Semi-logarithmic plots for photoproduct remaining *versus* time after

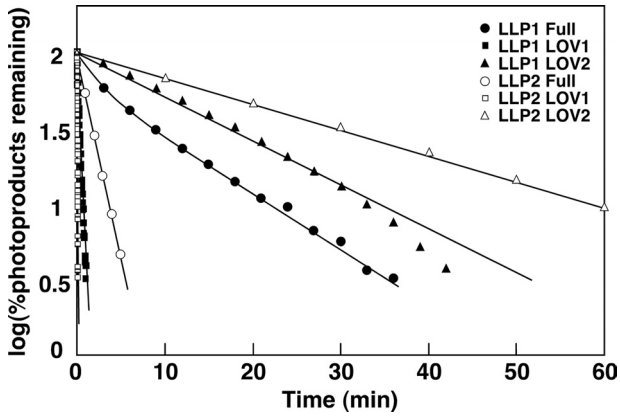


FIGURE 8. **Reaction kinetics for the dark recovery of the light-activated full-length and LOV domain proteins from *Pp*LLP1 and *Pp*LLP2.** The kinetic data were obtained by following the absorption changes at 450 nm in Fig. 7.

a light exposure (dark incubation time) were nearly log-linear for the single LOV domain proteins (Fig. 8), indicating that regeneration of the dark form is first order. The rate constants of dark recovery for *Pp*LLP1 LOV1 and LOV2 were 3.5 and $6.9 \times 10^{-2}$ min$^{-1}$, and those for *Pp*LLP2 LOV1 and LOV2 were 33 and $3.9 \times 10^{-2}$ min$^{-1}$, respectively. The dark recovery of the LOV1 domain is faster than that of the LOV2 domain in both *Pp*LLP1 and *Pp*LLP2. The dark recovery of the full-length LLP1 was slower than that of the LLP2.

## DISCUSSION

In this study, we demonstrate that LLPs are plant flavoproteins that undergo the typical photocycle of other LOV domain-containing proteins such as phototropins. Although the physiological function of LLPs remain unknown, homologous sequences have been found from *A. thaliana*, *S. lycopersicum*, *O. sativa*, and *P. patens* (as shown in Fig. 1*A*) and also from poplar (*Populus trichocarpa*), grapevine (*Vitis vinifera*), and the spikemoss *Selaginella moellendorffii* in their complete genome sequences by BLAST search (supplemental Fig. S2). When compared with amino acid sequences of LLPs from flowering plants and *P. patens*, not only the LOV domains but also the intervening sequences between LOV1 and LOV2 domains and the C-terminal extensions outside of LOV2 domains show significant similarities. This sequence conservation suggests that LLPs of flowering plants and *P. patens* are evolutionarily related. The amino acid at the position equivalent to the essential cysteine in the LOV1 domain of angiosperm LLPs is glycine or alanine, whereas that of the moss *P. patens* LLPs and the spikemoss *S. moellendorffii* LLP is cysteine (Fig. 1 and supplemental Fig. S2). The cysteine in the LOV1 domain seems to be lost in the evolution from spikemoss to angiosperm. The wide distribution implies that LLP may play a role in common physiological responses of plants.

*A. thaliana* LLP was first described in a review by Crosson *et al.* (17), referred to as PLP, and has been so far referred to as PLP in several studies (1, 18, 25). Because LOV domains are members of the large and diverse superfamily of PAS domains (2), the amino acid sequences of PAS and LOV domains resemble each other. In the case of *A. thaliana* LLP, the essential cysteine for photochemical reaction of LOV domains is not conserved in the LOV1, so that the N-terminal domain is recognized only as a PAS domain. However, a phylogenetic analysis clearly shows that the N-terminal domains of *A. thaliana* and *S. lycopersicum* LLPs are more closely related to LOV domains of phototropins than to PAS domains (Fig. 2). Thus, we propose that the N-terminal domains should be classified as LOV domains.

Only one amino acid replacement (G66C) restored LOV domain-like photochemistry in the LOV1 domain of *Sl*LLP. Amino acids required for the photochemical reaction have been maintained even in the absence of the cysteine. This fact suggests that LOV1 domains of angiosperm LLPs may have lacked the cysteine during their evolution. The LOV1 domains of *A. thaliana* phototropin 1 and 2 are proposed to function as a dimerization site for the phototropins (26). Interestingly, the dimer formation is light-independent (26). Therefore, a photochemical function of LOV1 domains may not be necessary to allow them to undergo protein-protein interaction. Although the LOV1 domain of *Sl*LLP does not show any light-induced spectral change, FMN binding in the LOV1 domain might be required to keep the proper three-dimensional structure for its dimerization function.

The molar ratio of FMN to protein for wild-type *Sl*LLP was 0.37 (supplemental Table S2), although we expected that it would become ~2 because *Sl*LLP contains two LOV domains. In addition to *Sl*LLP, all of the *Sl*LLP variants and all proteins derived from *Pp*LLP1 and *Pp*LLP2 showed low molar ratios compared with the value expected from the number of LOV domain having the potential FMN binding in each protein (supplemental Tables S2 and S3). However, the measured ratios of the proteins containing one potential FMN-binding LOV domain become roughly half of those containing two potential domains (supplemental Tables S2 and S3). In the case of phototropins, it has been shown that the ratios are 0.6 to 1.0 for single and 1.2 to 2.1 for double LOV domain-containing proteins (2). The low ratios could be due to low affinity of LOV domains of LLPs to FMN, and FMN could be released from the LOV domains during purification. It could also be possible that the capacity of FMN biosynthesis in *E. coli* cells is not sufficient to provide FMN to all expressed proteins. Although the protein samples used in this study include apoprotein without FMN, properties of FMN binding and light-dependent FMN-cysteinyl adduct formation are probably not affected by the presence of the apoprotein.

Imidazole accelerates the rate of dark reversion of *Sl*LLP (Fig. 5). The imidazole-dependent acceleration was also observed in *Pp*LLP1 and *Pp*LLP2 (supplemental Fig. S3). Alexandre *et al.* (23) have shown that, using LOV domains of phototropins, imidazole acts as base and catalyzes the dark reversion via abstraction of the proton from N5 position of the FMN-cysteinyl adduct. In LLPs, imidazole probably acts through the same mechanisms. The authors also suggest that a histidine can be involved in the tuning of the rate of dark reversion via a hydrogen bonding network from a surface-exposed histidine because of the absence of a histidine in the vicinity of FMN chromophore in *Avena sativa* PHOT1 LOV2 used for their experiments (23). The histidines of LLPs ($His^{340}$ of *Sl*LLP, $His^{370}$ of *Pp*LLP1, and $His^{383}$ of *Pp*LLP2), which are located at the posi-

tions equivalent to the above-mentioned surface-exposed histidine of *A. sativa* PHOT1 LOV2, could act as intrinsic base catalysts via a hydrogen bonding network. On the other hand, the histidine is not conserved even in the LOV domains that have been already recognized the imidazole-dependent acceleration of dark reversion: *Chlamydomonas reinhardtii* PHOT LOV2 (23) and cyanobacterial LOVs (All2875-LOV and Alr3170-LOV) (22). The imidazole-dependent acceleration may not be related to the presence of an intrinsic histidine involved in the dark reversion.

Ogura *et al.* (18) have shown that *At*LLP interacts with VTC2, VTC2L, BLH10A, and BLH10B in yeast two-hybrid systems. The interactions with VTC2L, BLH10A, and BLH10B are specifically diminished by blue light irradiation in yeast cells, suggesting that LLP may function as a photoreceptor (18). The LOV2 domain of *A. thaliana* phototropin 2 binds to its C-terminal Ser/Thr kinase domain in the dark and inhibits the kinase activity (27). When irradiated with light, LOV2 domain dissociates from the kinase domain so that the kinase activity is activated (27). Because LLPs do not contain effector domains in themselves, unlike phototropins, binding proteins such as those mentioned above may be working as effectors.

The photochemical properties of LLPs shown in this study indicate that LLP family proteins have the potential to function in light perception. As a next step, it is important to elucidate the biological function of LLPs. Making gene disruptions of *P. patens* and studying phenotypes of the gene disruptants may reveal their possible photoreceptor roles.

*Acknowledgment—We thank Dr. Winslow Briggs (Carnegie Institution for Science) for helpful comments and critical reading of the manuscript.*

## REFERENCES


1. Christie, J. M. (2007) *Annu. Rev. Plant Biol.* **58,** 21–45
2. Christie, J. M., Salomon, M., Nozue, K., Wada, M., and Briggs, W. R. (1999) *Proc. Natl. Acad. Sci. U.S.A.* **96,** 8779–8783
3. Salomon, M., Christie, J. M., Knieb, E., Lempert, U., and Briggs, W. R. (2000) *Biochemistry* **39,** 9401–9410
4. Kasahara, M., Swartz, T. E., Olney, M. A., Onodera, A., Mochizuki, N., Fukuzawa, H., Asamizu, E., Tabata, S., Kanegae, H., Takano, M., Christie, J. M., Nagatani, A., and Briggs, W. R. (2002) *Plant Physiol.* **129,** 762–773
5. Kottke, T., Hegemann, P., Dick, B., and Heberle, J. (2006) *Biopolymers* **82,** 373–378
6. Briggs, W. R. (2007) *J. Biomed. Sci.* **14,** 499–504
7. Tokutomi, S., Matsuoka, D., and Zikihara, K. (2008) *Biochim. Biophys. Acta* **1784,** 133–142
8. Schwerdtfeger, C., and Linden, H. (2003) *EMBO J.* **22,** 4846–4855
9. Takahashi, F., Yamagata, D., Ishikawa, M., Fukamatsu, Y., Ogura, Y., Kasahara, M., Kiyosue, T., Kikuyama, M., Wada, M., and Kataoka, H. (2007) *Proc. Natl. Acad. Sci. U.S.A.* **104,** 19625–19630
10. Swartz, T. E., Tseng, T. S., Frederickson, M. A., Paris, G., Comerci, D. J., Rajashekara, G., Kim, J. G., Mudgett, M. B., Splitter, G. A., Ugalde, R. A., Goldbaum, F. A., Briggs, W. R., and Bogomolni, R. A. (2007) *Science* **317,** 1090–1093
11. Purcell, E. B., Siegal-Gaskins, D., Rawling, D. C., Fiebig, A., and Crosson, S. (2007) *Proc. Natl. Acad. Sci. U.S.A.* **104,** 18241–18246
12. Somers, D. E., Schultz, T. F., Milnamow, M., and Kay, S. A. (2000) *Cell* **101,** 319–329
13. Nelson, D. C., Lasswell, J., Rogg, L. E., Cohen, M. A., and Bartel, B. (2000) *Cell* **101,** 331–340
14. Schultz, T. F., Kiyosue, T., Yanovsky, M., Wada, M., and Kay, S. A. (2001) *Plant Cell* **13,** 2659–2670
15. Imaizumi, T., Tran, H. G., Swartz, T. E., Briggs, W. R., and Kay, S. A. (2003) *Nature* **426,** 302–306
16. Sakai, T., Kagawa, T., Kasahara, M., Swartz, T. E., Christie, J. M., Briggs, W. R., Wada, M., and Okada, K. (2001) *Proc. Natl. Acad. Sci. U.S.A.* **98,** 6969–6974
17. Crosson, S., Rajagopal, S., and Moffat, K. (2003) *Biochemistry* **42,** 2–10
18. Ogura, Y., Komatsu, A., Zikihara, K., Nanjo, T., Tokutomi, S., Wada, M., and Kiyosue, T. (2008) *J. Plant Res.* **121,** 97–105
19. Higuchi, R., Krummel, B., and Saiki, R. K. (1988) *Nucleic. Acids Res.* **16,** 7351–7367
20. Ishikawa, M., Takahashi, F., Nozaki, H., Nagasato, C., Motomura, T., and Kataoka, H. (2009) *Planta* **230,** 543–552
21. Crosson, S., and Moffat, K. (2001) *Proc. Natl. Acad. Sci. U.S.A.* **98,** 2995–3000
22. Narikawa, R., Zikihara, K., Okajima, K., Ochiai, Y., Katayama, M., Shichida, Y., Tokutomi, S., and Ikeuchi, M. (2006) *Photochem. Photobiol.* **82,** 1627–1633
23. Alexandre, M. T., Arents, J. C., van Grondelle, R., Hellingwerf, K. J., and Kennis, J. T. (2007) *Biochemistry* **46,** 3129–3137
24. Fedorov, R., Schlichting, I., Hartmann, E., Domratcheva, T., Fuhrmann, M., and Hegemann, P. (2003) *Biophys. J.* **84,** 2474–2482
25. Ogura, Y., Tokutomi, S., Wada, M., and Kiyosue, T. (2008) *Plant Signal Behav.* **3,** 966–968
26. Katsura, H., Zikihara, K., Okajima, K., Yoshihara, S., and Tokutomi, S. (2009) *FEBS Lett.* **583,** 526–530
27. Matsuoka, D., and Tokutomi, S. (2005) *Proc. Natl. Acad. Sci. U.S.A.* **102,** 13337–13342
28. Finn, R. D., Mistry, J., Tate, J., Coggill, P., Heger, A., Pollington, J. E., Gavin, O. L., Gunasekaran, P., Ceric, G., Forslund, K., Holm, L., Sonnhammer, E. L., Eddy, S. R., and Bateman, A. (2010) *Nucleic Acids Res.* **38,** D211–D222